Heterobimetallic Indenyl Complexes. Synthesis and Carbonylation Reaction of *anti*-[Cr(CO)$_3$-μ,η:η-indenyl-Ir(COD)]

Pierluigi Cecchetto, Alberto Ceccon,* Alessandro Gambaro, and Saverio Santi

Dipartimento di Chimica Fisica, Università di Padova, Via Loredan 2, 35131 Padova, Italy

Paolo Ganis

Dipartimento di Chimica, Università di Napoli, Via Mezzocannone 4, 80134 Napoli, Italy

Roberto Gobetto

Dipartimento di Chimica Inorganica, Chimica Fisica e Chimica dei Materiali, Università di Torino, Via Giuria 7, 10125 Torino, Italy

Giovanni Valle

CNR, Centro di Studio sui Biopolimeri, Via Marzolo 3, 35131 Padova, Italy

Alfonso Venzo

CNR, Centro di Studio sugli Stati Molecolari Radicalici ed Eccitati, Via Loredan 2, 35131 Padova, Italy

Received July 17, 1997

The reaction of the *anti*-[Cr(CO)$_3$-μ,η:η-indenyl-Ir(COD)] (**I**) complex with an excess of CO in CH_2Cl_2 at 203 K produces quantitatively the η^1-[η^6-Cr(CO)$_3$-indenyl]-Ir(COD)(CO)$_2$ intermediate which above 273 K converts into the fully carbonylated complex η^1-[η^6-Cr(CO)$_3$-indenyl]Ir(CO)$_4$; this in turn is stable up to 313 K. Carbonylation of the *anti*-[Cr(CO)$_3$-μ,η:η-indenyl-Ir(COE)$_2$] analogue (**II**) gives the η^1-[η^6-Cr(CO)$_3$-indenyl]-Ir(CO)$_4$ (**VII**) species in a single fast step. In contrast to the behavior of the corresponding rhodium complexes, for which η^1 intermediates have never been observed and the aromatized substitution product is the stable product, the rearomatization of the cyclopentadienyl ring in iridium complexes to give the "normal" substitution product, viz., *anti*-[Cr(CO)$_3$-μ,η:η-indenyl-Ir(CO)$_2$] (**III**) is a difficult process which takes place only on bubbling argon through the solution. The final product **III** is barely stable in solution. If the carbonylation is carried out using a blanket of CO over the solution of complexes **I** and **II**, viz., failing CO, the scarcely soluble iridium dimer [η^6-Cr(CO)$_3$-indenyl-η^3-Ir(CO)$_3$]$_2$ (**IX**) stable in the solid state is obtained, probably by dimerization of the unstable intermediate *anti*-[η^6-Cr(CO)$_3$-indenyl-η^3-Ir(CO)$_3$] (**X**).

Introduction

η^5-Indenyl-ML$_2$ (M = Co, Rh, Ir, etc.) complexes are far more reactive than the corresponding cyclopentadienyl analogues in substitution reactions of the ancillary ligands with nucleophiles.[1] For example, easy substitution of two CO's for COD takes place at room temperature in η-indenyl-M(COD), whereas forced conditions, viz., high temperature and high CO pressure, are required in the case of the corresponding cyclopentadienyl complexes. This enhanced reactivity was attributed to an easier metal slippage to form lower hapticity η^3 or η^1 intermediates, which are energetically favored in the case of indenyl complexes because of concomitant aromatization of the fused benzene ring. As a matter of fact, direct evidence for the formation of an η^3 intermediate along the substitution path in both Rh and Ir complexes is still elusive, even though its postulation is sometimes necessary to explain the kinetic data and the reaction products.[2] In contrast, there is direct experimental evidence for the presence of an η^1 species as an intermediate in the associative substitution reaction of COD with carbon monoxide in η^5-indenyl-Ir(COD).[3] Below 243 K, the reagent is transformed into the stable η^1-indenyl-Ir(COD)(CO)$_2$

(1) (a) Rerek, M. E.; Basolo, F. *Organometallics* **1983**, *2*, 372. (b) Moreno, C.; Macazaga, M. J.; Delgado, S. *Organometallics* **1991**, *10*, 1124. (c) Cheong, M.; Basolo, F. *Organometallics* **1988**, *7*, 2041. (d) Rerek, M. E.; Basolo, F. *J. Am. Chem. Soc.* **1984**, *106*, 5908. (e) Kakkar, A. K.; Taylor, N. J.; Marder, T. B.; Shen, J. K.; Hallinan, N.; Basolo, F. *Inorg. Chim. Acta* **1992**, *198*−*200*, 219.

(2) (a) Rerek, M. E.; Ji, L. N.; Basolo, F. *J. Chem. Soc., Chem. Commun.* **1983**, 1208. (b) Wescott, S. A.; Kakkar, A. K.; Stringer, S.; Taylor, N. J.; Marder, T. B. *J. Organomet. Chem.* **1990**, *394*, 777.

(3) Bellomo, S.; Ceccon, A.; Gambaro, A.; Santi, S.; Venzo, A. *J. Organomet. Chem.* **1993**, *453*, C4−C6.

S0276-7333(97)00606-7 CCC: $15.00
Publication on Web 01/22/1998

species which, on raising the temperature, is quantitatively converted into η^5-indenyl-Ir$(CO)_2$. This $\eta^1 \rightarrow \eta^5$ rearrangement, involving the loss of the two π bonds between the metal and COD and the restoration of the aromaticity of the fused Cp ring, exhibits a relatively high enthalpy of activation ($\Delta H^{\ddagger} = 79$ kJ mol^{-1}). In the carbonylation reaction of the analogous η^5-indenyl-Rh(COD) complex no η^1 species was observed even at very low temperature (−80 °C), indicating that if the potential η^1-indenyl-Rh(COD)$(CO)_2$ intermediate is formed, it probably loses COD and restores the η^5 coordination mode much faster than the iridium complex.[4]

In recent years we have been developing the chemistry of bimetallic indenylrhodium complexes in which the benzene ring is π-bonded to the Cr$(CO)_3$ group in a *syn* or *anti* stereochemistry.[5] We have found that the rate of substitution of the ancillary ligands at rhodium increases to a great extent if the benzene ring is coordinated to Cr$(CO)_3$ in a *transoid* arrangement. In particular, we have been studying the kinetics of the carbonyl substitution at rhodium with COD and NBD in *anti*-[Cr$(CO)_3$-μ,η:η-indenyl-Rh$(CO)_2$] and have suggested an η^1-indenylrhodium species as the most probable intermediate along the reaction pathway.[4] Conversely, the *syn* coordination with Cr$(CO)_3$ did not induce significant changes in the substitution rate of CO's.

Since the third transition series elements generally stabilize low-hapticity species to a greater extent than the corresponding metals of the second series, we undertook a study concerning the synthesis and the reactivity of some bimetallic Cr$(CO)_3$-μ,η:η-indenyl-IrL_2 complexes with the aim of observing the corresponding η^1-iridium intermediates. We were particularly interested in the chemical behavior of *anti*-[Cr$(CO)_3$-μ,η:η-indenyl-Ir(COD)] in the presence of carbon monoxide. Addition or loss of CO to or from a metal center represents a crucial step in many transition metal-catalyzed processes, and a comparison between the iridium and rhodium species in this kind of reaction under particularly mild conditions seemed promising.

Results and Discussion

Metalation of indene, carried out at room temperature by treatment with KH of its THF solution, produced the indenyl anion potassium salt. Successive quenching of the anionic solution with [Ir$(L)_2(\mu$-Cl)$]_2$ or [Ir$(L_2)(\mu$-Cl)$]_2$ (L = cyclooctene (COE), L_2 = 1,5-cyclooctadiene (COD)) afforded the corresponding η^5-indenyl-Ir$(COE)_2$ and η^5-indenyl-Ir(COD) complexes in agreement with published procedures.[6] Both complexes react easily with CO (1 bar) at room temperature to give η^5-indenyl-Ir$(CO)_2$ in quite good yield. The results of a study dealing with the mechanism of this olefin substitution reaction have been reported.[3]

Heterobimetallic chromium−iridium indenyl complexes were prepared by using an analogous procedure. In order to avoid the $\eta^6 \rightarrow \eta^5$ haptotropic migration of the Cr$(CO)_3$ group, η^6-indene-Cr$(CO)_3$ was metalated in THF with KH at −40 °C.[7] Quenching of the solution with the appropriate iridium dimer afforded the bimetallic *anti*-[Cr$(CO)_3$-μ,η:η-indenyl-Ir(COD)] (**I**) or *anti*-[Cr$(CO)_3$-μ,η:η-indenyl-Ir$(COE)_2$] (**II**) complexes. We attributed the *anti* stereochemistry to both products because of the close similarity of their ^{1}H and ^{13}C NMR spectral parameters with those of the corresponding chromium−rhodium complexes. For **I**, the *anti* location of the two inorganic units was also confirmed by X-ray analysis (see below).

In analogy with substitution rates of the ancillary ligands in the corresponding rhodium complexes, we expected that substitution of COD or COE by CO in the bimetallic complexes **I** and **II** would take place faster than in the monometallic η^5-indenyl-IrL_2. As a matter of fact, carbonylation of **I** and **II** proceeds differently from that of the monometallic complexes, and a detailed description of the process will be reported below. Since preparation and isolation of pure *anti*-[Cr$(CO)_3$-μ,η:η-indenyl-Ir$(CO)_2$] (**III**) was not feasible by direct reaction of **I** or **II** with CO, we explored the complexation of monometallic η^5-indenyl-Ir$(CO)_2$ with Cr$(CO)_3$ as an alternative synthetic procedure. The reaction of this complex with $(CH_3CN)_3Cr(CO)_3$ in THF for 5 h at 25 °C afforded an orange-red compound the elemental analysis of which corresponds to that of the expected product. The IR spectrum shows two bands at 2046 and 1984 cm^{-1} due to the stretching modes of the CO groups bonded to iridium and two bands at 1944 and 1895 cm^{-1} due to the tricarbonylchromium tripod. The ^{1}H NMR spectrum (submitted as Supporting Information) and the ^{13}C NMR parameters (see Experimental Section) of this compound show that the chemical shift values of the indenyl frame resemble more closely those of *syn*-[Cr$(CO)_3$-μ,η:η-indenyl-RhL_2] complexes[5b,c] rather than those of *anti*-[Cr$(CO)_3$-μ,η:η-indenyl-RhL_2] complexes.[8] X-ray analysis (see below) showed that the two metals are situated in the *syn* configuration giving rise to *syn*-[Cr$(CO)_3$-μ,η:η-indenyl-Ir$(CO)_2$] (**IV**). The expected *anti* isomer, **III**, was not detected. Complex **III** was obtained only in solution as an unstable species by a different route and its formation and spectroscopic characterization will be presented below. It must be mentioned that complexation of the benzene ring of the monometallic η^5-indenyl-Ir$(CO)_2$ complex with Cr$(CO)_3$ takes place under milder conditions than in the case of most aromatic hydrocarbons usually requiring much higher temperatures for complexation (T > 100 °C). This behavior is likely due to a significant decrease in aromatic character of the six-membered ring whose π electrons are in part engaged in the coordination with iridium. As a consequence, electronic structures where the six-membered ring exhibits a pronounced diene character become important (cf. the X-ray analysis), and therefore, complexation with Cr$(CO)_3$ would take place easily via the formation of an η^4 intermediate. This species appears to be particularly stable in the case of bimetallic systems as suggested by recent results con-

(4) Bonifaci, C.; Carta, G.; Ceccon, A.; Gambaro, A.; Santi, S.; Venzo, A. *Organometallics* **1996**, *15*, 1630.

(5) (a) Ceccon, A.; Gambaro, A.; Santi, S.; Valle, G.; Venzo, A. *J. Chem. Soc., Chem. Commun.* **1989**, 51. (b) Bonifaci, C.; Ceccon, A.; Gambaro, A.; Ganis, P.; Santi, S.; Valle, G.; Venzo, A. *Organometallics* **1993**, *12*, 4211. (c) Bonifaci, C.; Ceccon, A.; Gambaro, A.; Ganis, P.; Santi, S.; Valle, G.; Venzo, A. *J. Organomet. Chem.* **1995**, *492*, 35.

(6) Merola, J. S.; Kackmarcik, R. T. *Organometallics* **1989**, *8*, 778.

(7) Ceccon, A.; Gambaro, A.; Gottardi, F.; Santi, S.; Venzo, A. *J. Organomet. Chem.* **1991**, *412*, 85.

(8) (a) Ceccon, A.; Gambaro, A.; Santi, S.; Venzo, A. *J. Mol. Catal.* **1991**, *69*, L1−L6. (b) Ceccon, A.; Elsevier, C. J.; Ernsting, J. M.; Gambaro, A.; Santi, S.; Venzo, A. *Inorg. Chim. Acta* **1993**, *204*, 15.

Table 1. Selected Bond Lengths, Bond Angles, and Geometrical Parameters for the Complexes *anti*-[Cr(CO)$_3$-indenyl-Ir(COD)] (I), *syn*-[Cr(CO)$_3$-indenyl-Ir(CO)$_2$] (IV), and indenyl-Ir(COD) (V)

	I	IV	V
	Bond Lengths/Å		
Ir−C(1)	2.26(1)	2.25(2)	2.211(9)
Ir−C(2)	2.26(2)	2.26(2)	2.23(1)
Ir−C(3)	2.24(2)	2.23(2)	2.23(1)
Ir−C(3a)	2.36(2)	2.59(2)	2.372(9)
Ir−C(7a)	2.34(2)	2.56(2)	2.38(1)
Cr−C(3a)	2.33(2)	2.34(2)	
Cr−C(4)	2.21(2)	2.25(2)	
Cr−C(5)	2.20(2)	2.17(2)	
Cr−C(6)	2.19(2)	2.19(2)	
Cr−C(7)	2.24(3)	2.23(2)	
Cr−C(7a)	2.41(2)	2.42(2)	
Ir−Cr		3.068(3)	
C(1)−C(2)	1.44(3)	1.45(2)	1.45(2)
C(2)−C(3)	1.44(3)	1.45(2)	1.45(2)
C(1)−C(7a)	1.40(3)	1.43(2)	1.41(2)
C(3)−C(3a)	1.43(2)	1.50(2)	1.41(1)
C(3a)−C(7a)	1.50(3)	1.45(2)	1.46(1)
C(3a)−C(4)	1.48(3)	1.40(2)	1.40(1)
C(4)−C(5)	1.32(2)	1.42(2)	1.37(2)
C(5)−C(6)	1.41(3)	1.37(3)	1.38(2)
C(6)−C(7)	1.43(3)	1.53(3)	1.39(2)
C(7)−C(7a)	1.40(3)	1.38(3)	1.44(2)
	Bond Angles/deg		
Cr−C(8)−O(8)	174(1)	171(1)	
Cr−C(9)−O(9)	178(2)	179(2)	
Cr−C(10)−O(10)	178(1)	177(1)	
C(8)−Cr−C(9)	89(1)	85.7(8)	
C(8)−Cr−C(10)	88(1)	95.5(8)	
C(9)−Cr−C(10)	89(1)	84.6(8)	
Ir−C(11)−O(11)		176(2)	
Ir−C912)−O(12)		176(1)	
	Parameters		
Δ(M−C)/Å	0.10	0.33	0.15
HA/deg	5.8	17	8.6

cerning the exchange of the Cr(CO)$_3$ unit with cycloheptatriene in bimetallic chromium−rhodium indenyl complexes.[4] At present we cannot explain the exclusive formation of the *syn* isomer in any other way than by comparison with the analogous indenyl complexes of rhodium. For this class of compounds, at least with norbornadiene as the ancillary ligand, the *syn* isomer is thermodynamically more stable than the *anti* isomer, even though its structure requires severe molecular constraints.[5b,9]

X-ray Measurements. Crystals useful for diffractometric analysis were obtained by slow evaporation of concentrated solutions of η^5-indenyl-Ir(COD) (**V**), **I**, and **IV**. Selected bond distances and the values of the parameters conventionally adopted in order to describe the metal coordination modes to arene ligands, i.e., ring slip distortion (Δ(M−C)) and hinge angle (HA),[10] are reported in Table 1. A perspective view of the structures of **IV** is shown in the Figure 1 (those of **I** and **V** are given as Supporting Information). In the monometallic complex **V**, taken as a reference species, the distances from iridium to the carbon atoms of the five-membered

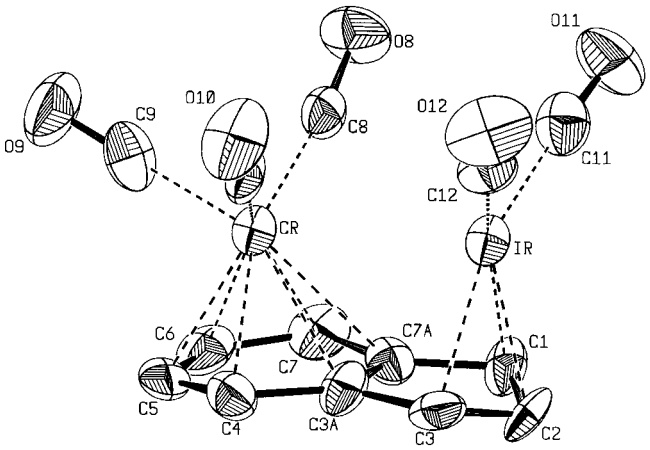

Figure 1. ORTEP view of *syn*-[Cr(CO)$_3$-μ,η:η-indenyl-Ir(CO)$_2$] (**IV**).

ring indicate a slightly distorted η^5 coordination of the metal similar to that found for several others monometallic indenyl complexes.[2b,10] The distortion arises from the puckering of the [C$_1$,C$_2$,C$_3$] plane with respect to the remainder of the indenyl skeleton (HA = 8.6°), and the distances of the metal from the C$_{3a}$,C$_{7a}$ ring junction carbons are only little longer than those from C$_1$, C$_2$, and C$_3$ (i.e., Δ(M−C) = 0.15 Å). This situation is not significantly modified by coordination of the six-membered ring with Cr(CO)$_3$ in the *anti* arrangement. In fact, in the *anti* complex **I**, both the puckering of the cyclopentadienyl ring (HA = 5.8°) and the slippage of iridium toward the external C$_1$, C$_2$, and C$_3$ carbon atoms (Δ(M−C) = 0.10 Å) are only slightly lower with respect to the monometallic complex **V**. Moreover, the chromium−carbon bond distances indicate a small slippage of chromium from the ideal η^6 hapticity toward an η^4 one. As already observed in the analogous rhodium complexes, *anti* coordination of the benzene ring with Cr(CO)$_3$ does not modify significantly the geometrical parameters of the *ortho*-condensed CpML$_2$ subunit; this similarity in structure, however, does not translate into similarity in reactivity in those reactions where rhodium is directly involved, the bimetallic complexes being much more reactive than the monometallic ones. We expected to record a similar trend in iridium compounds.

As shown in Figure 1, the two metals in **IV** are located on the same side of the indenyl plane. The parameters that describe the coordination mode of iridium to the Cp ring differ significantly from those of the other two complexes, **I** and **V**; the geometric distortions observed for the *syn* isomer are noticeably higher than those for the *anti* isomer, the value of HA changing from 5.8 to 17°, and that of Δ(M−C) from 0.10 to 0.32 Å. These data suggest a remarkable shift of iridium toward an η^3 hapticity. At the same time, the position of chromium does not differ significantly between the *anti* and *syn* complexes, as shown by the similar values of chromium−carbon distances found in both cases, suggesting that the slippage of iridium toward the external carbon atoms of the five-membered ring is likely induced by electronic rather than steric reasons.

The NMR results show that the difference between the structural features of **I** and **IV** persists also in solution. Taking the monometallic η^5-indenyl-Ir(CO)$_2$ as reference, the minor coordinative engagement of C$_{3a}$

(9) Bonifaci, C.; Ceccon, A.; Gambaro, A.; Ganis, P.; Santi, S.; Valle, G.; Venzo, A. *Organometallics* **1995**, *14*, 2430.

(10) (a) Merola, J. S.; Kackmarcik, R. T.; Van Engen, D. *J. Am. Chem. Soc.* **1986**, *108*, 329. (b) Marder, T. B.; Calabrese, J. C.; Roe, D. C. *Organometallics* **1987**, *6*, 2012. (c) Kakkar, A. K.; Jones, S. F.; Taylor, N. J.; Collins, S.; Marder, T. B. *J. Chem. Soc., Chem. Commun.* **1989**, 1454.

and C_{7a} in **IV** with respect to **I** is suggested by the effect of complexation with $Cr(CO)_3$ on their chemical shift ($\Delta\delta = \delta_{complex} - \delta_{free} = -5.65$ ppm), which is close to that found for the analogous *syn* rhodium complexes ($\Delta\delta = -8.29$ ppm).[5b] On the other hand, the $Cr(CO)_3$ complexation effects on quaternary carbon atoms are substantially larger in the case of *anti*-[$Cr(CO)_3$-μ,η:η-indenyl-$Ir(CO)_2$] ($\Delta\delta = -25.23$ ppm; see below), as well as in a wide series of *anti*-(Cr,Rh)-indenyl complexes (mean value is $\Delta\delta \cong -26.6$ ppm)[8b] and, in general, in substituted arenes (mean value is $\Delta\delta \cong -28$ ppm).[11] Moreover, the tetrahedralization of the C_4 and C_7 carbon atoms is evidenced by the much more pronounced upfield shift of the resonances of the nuclei located in these pivot positions with respect to those of the nuclei in positions 5 and 6, as shown by comparing the NMR data for η^5-indenyl-$Ir(CO)_2$ and **IV** [$\Delta\delta(C_4,C_7) = -46.86$ ppm, $\Delta\delta(C_5,C_6) = -36.42$ ppm; $\Delta\delta(H_4,H_7) = -3.1$ ppm, $\Delta\delta(H_5,H_6) = -1.9$ ppm]. The increase of the hinge angle from 8.6° in η^5-indenyl-$Ir(CO)_2$ to 17° in **IV** is also in agreement with the observed large negative value of $\Delta\delta$-(C_1,C_3) (−19.5 ppm). Conversely, the complexation effects of an *anti* $Cr(CO)_3$ group on the ^1H and ^{13}C NMR parameters are markedly lower, and their values are very close to those observed for the analogous *anti*-[Cr-$(CO)_3$-μ,η:η-indenyl-RhL_2] complexes.[5,8,9]

Reaction of I and II with Carbon Monoxide. (a) η^1-[η^6-$Cr(CO)_3$-indenyl]-IrL_4 Complexes. On bubbling CO through a CH_2Cl_2 solution of **I** at 203 K (so attaining a very large excess CO) the color changes suddenly from orange to dark yellow. The solution shows two IR bands at 2036.2 and 1989.8 cm^{-1}, due to the stretching modes of the CO ligands bonded to iridium, and two strong absorptions at 1950.5 and 1870.1 cm^{-1}, typical of the $Cr(CO)_3$ group (see Figure 2a). The ^1H NMR spectrum recorded at the same temperature shows the absence of signals due to complex **I**, and a new ABCDMNX pattern, characteristic of an indene residue, appears (see Figure 3, trace A). The COD ligand appears still coordinated to iridium as indicated by the signals of its vinyl hydrogens at ∼3.9 and 4.1 δ, that is ∼1.5 ppm upfield with respect to the resonance range of the free olefin. Thus, in analogy to the behavior of the monometallic η^5-indenyl-Ir(COD) complex,[3] we attribute the η^1-[η^6-$Cr(CO)_3$-indenyl]-Ir-$(COD)(CO)_2$ structure **VI** to this species; the signals of the olefinic COD protons appear as two distinct multiplets due to the chiral nature of the η^1-indene ligand.

VI is stable until 273 K; above this temperature, the intensity of the IR bands at 2036 and 1990 cm^{-1} diminishes until their disappearance and three new absorptions grow at 2118.3, 2051.4, and 2024.1 cm^{-1} (cf. Figure 2b). Moreover, the bands characteristic of the $Cr(CO)_3$ tripod are only slightly shifted to 1955.4 and 1876.4 cm^{-1}. The ^1H NMR spectrum (recorded at 203 K) of the final solution (Figure 3, trace B) shows again the pattern characteristic for an indene residue; however, in this case, the resonance of COD olefinic protons at 5.57 δ indicates that the olefin is no longer coordinated to iridium. We believe that the reaction of **VI** with excess CO present in solution affords complex **VII** where the $Ir(CO)_4$ moiety is still η^1-bonded to the indene residue.

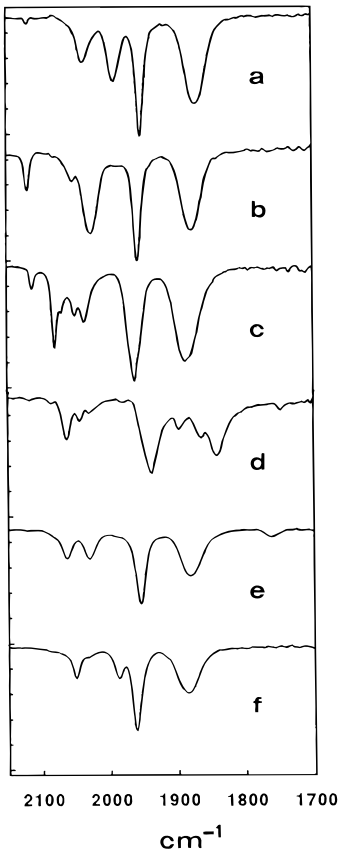

Figure 2. IR spectra (solvent, CH_2Cl_2) of η^1-[η^6-$Cr(CO)_3$-indenyl]-$Ir(CO)_2$(COD) (**VI**) at 203 K (trace a), *ax*-η^1-[η^6-$Cr(CO)_3$-indenyl]-$Ir(CO)_4$ (**VII**-ax) at 273 K (trace b), *eq*-η^1-[η^6-$Cr(CO)_3$-indenyl]-$Ir(CO)_4$ (**VII**-eq) at 298 K (trace c), [η^6-$Cr(CO)_3$-indenyl-η^3-$Ir(CO)_3$]$_2$ (**IX**) at 213 K (trace d), [Cr-$(CO)_3$-indenyl-μ,η:η-$Ir(CO)_2$]$_2$ (**XI**) at 213 K (trace e), and *anti*-[$Cr(CO)_3$-μ,η:η-indenyl-$Ir(CO)_2$] (**III**) at 298 K (trace f). For other experimental conditions, see the text.

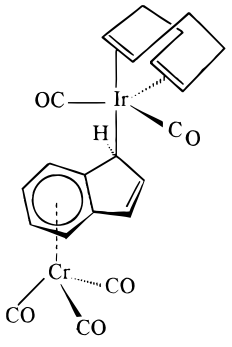

VI

The strong downfield shift exhibited by the signal of H_1 on going from **VI** to **VII** ($\Delta\delta = 1.48$ ppm) is in agreement with a higher number of carbonyls bonded to iridium. In the range of temperatures between 233 and 298 K, both IR and ^1H NMR spectra of the CD_2Cl_2 solution of **VII** change because of the occurrence of two intramolecular rearrangements described below.

It must be mentioned that on reacting **II** with CO under the same experimental conditions used with

(11) (a) Ceccon, A.; Gambaro, A.; Manoli, F.; Venzo, A.; Kuck, D.; Bitterwolf, T. E.; Ganis, P.; Valle, G. *J. Chem. Soc., Perkin Trans 2* **1991**, 233. (b) Ceccon, A.; Gambaro, A.; Manoli, F.; Venzo, A.; Kuck, D.; Ganis, P.; Valle, G. *J. Chem. Soc., Perkin Trans. 2* **1992**, 1111. (c) Ceccon, A.; Gambaro, A.; Manoli, F.; Venzo, A.; Ganis, P.; Valle, G.; Kuck, D. *Chem. Ber.* **1993**, *126*, 2053.

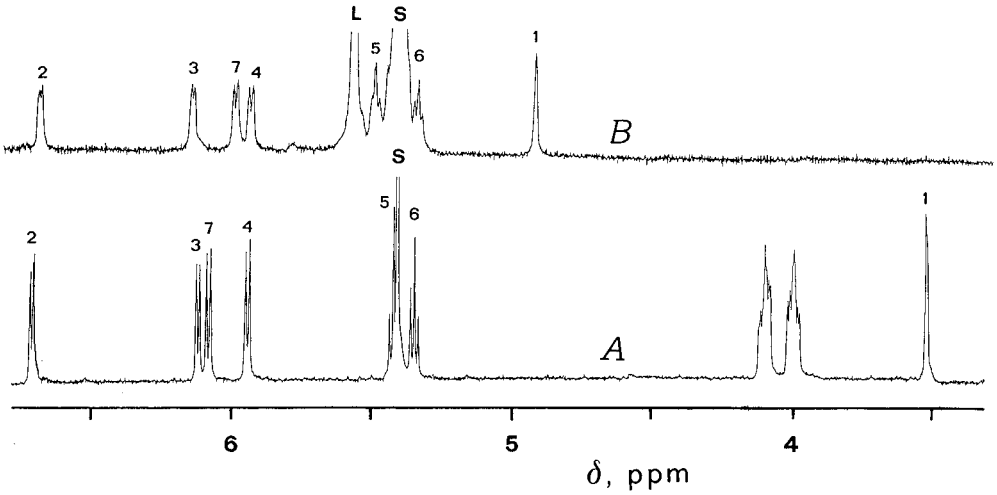

Figure 3. ^{1}H NMR spectra of η^1-[η^6-Cr(CO)$_3$-indenyl]-Ir(CO)$_2$(COD) (**VI**) (trace A), and η^1-[η^6-Cr(CO)$_3$-indenyl]-Ir(CO)$_4$ (**VII**) (trace B). L indicates the resonance of the olefinic protons of the free COD. For experimental conditions, see the text. The signal at δ 5.32 is due to the undeuterated part of the solvent. The signals due to the methylene protons of COD in **VI** are not reported.

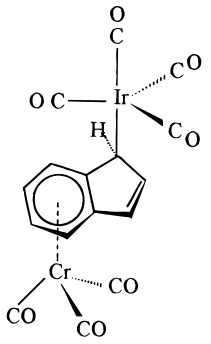

VII

complex **I**, one observes only the formation of **VII**. From these results, it is evident that in this case CO addition and COE elimination are indistinguishable processes even at 203 K.

It seems appropriate to compare the thermal stability and chemical behavior of the monometallic η^1-indenyl-Ir(COD)(CO)$_2$ intermediate, **VIII**, with that of **VI**. In fact, **VIII** already loses COD at 253 K to be quantitatively converted into η^5-indenyl-Ir(CO)$_2$,[3] whereas the bimetallic complex **VI** is thermally more stable and it is preferably converted into **VII**, which in turn is stable up to ~313 K. Thus, in bimetallic **VI** the substitution of COD with CO is an easier process than loss of COD to form the η^5-indenyl complex. As already reported,[4] the complexation of the indenyl ligand with Cr(CO)$_3$ stabilizes those species in which the second metal (rhodium or iridium) is coordinated to the five-membered ring with the lowest hapticity mode.

In spite of this, we have obtained the rearomatized product **III** by bubbling argon at room temperature through a CD_2Cl_2 solution of **VII**. Complex **III** is not very stable in solution, and attempts to isolate it in solid state failed. Its characterization was accomplished by analysis of the IR (Figure 2f) and NMR spectra of the argon-purged solution. The *anti* configuration of **III** was established on the basis of the close similarity of its spectral parameters (see Experimental Section) with those of the analogous *anti*-[Cr(CO)$_3$-μ,η:η-indenyl-Rh(CO)$_2$] complex,[8] and of the marked difference from those of the *syn* isomer **IV** (The ^{1}H NMR spectra of **I** and **IV** are given as Supporting Information).

(b) Dimeric Iridium Carbonyl Complexes. Dimeric iridium carbonyl complexes were obtained in different carbonylation conditions. Instead of bubbling CO through the solutions of complexes **I** and **II** as in the previous experiment, the same solutions were kept under a blanket of CO for a few minutes at room temperature so realizing a lower CO concentration. The color changed suddenly from orange to dark brown, and a yellow solid, **IX**, precipitated in 50% yield. The solid is stable under argon and its IR spectrum, recorded as a Nujol dispersion (Figure 4, trace A), exhibits three strong bands which have been assigned to the terminal CO's bonded to iridium (2090, 2070, and 2040 cm^{-1}) two bands (1746 (sh) and 1740 cm^{-1}) in the region of bridging Ir−CO's and five bands (1950 (sh), 1940, 1885, 1865 and 1840 cm^{-1}) due to the CO's bonded to chromium. The *syn* structure of **IX** fully justifies the number of active CO stretchings if we consider the Ir$_2$(CO)$_6$ and the Cr(CO)$_3$···Cr(CO)$_3$ systems each one belonging to the same vibrating system. Both have a C_{2v} local symmetry that provides three and two active ν(C≡O) modes for the terminal and bridged carbonyls of iridium and five for the chromium CO's. On the contrary, an *anti* conformation should impose a C_{2h} local symmetry providing in the above given order two, one, and three active ν(C≡O) modes which are less than those experimentally observed.[12] The assignment of bands to the different types of carbonyls was confirmed by the IR spectrum of the product obtained using ^{13}C-labeled CO as reagent (see Figure 4, trace B). The bands attributed to the carbonyls coordinated to iridium are shifted ~40 cm^{-1} to lower frequencies because of the isotope effect whereas those of tricarbonylchromium do not change. This demonstrates that both terminal and bridging CO's bonded to iridium arise from the

(12) One of the reviewers suggested that, given the likely inequivalence in the solid state arising from the crystal packing, the molecular symmetry in **IX** could be broken so either a *syn* or *anti* structure could be consistent with the reported number of the chromium and iridium carbonyl bands. The identical number of CO bands observed in the IR spectrum of **IX** either in solution (Figure 2d) or in solid (as a Nujol dispersion, Figure 4A) seems not to be in accord with his interpretation.

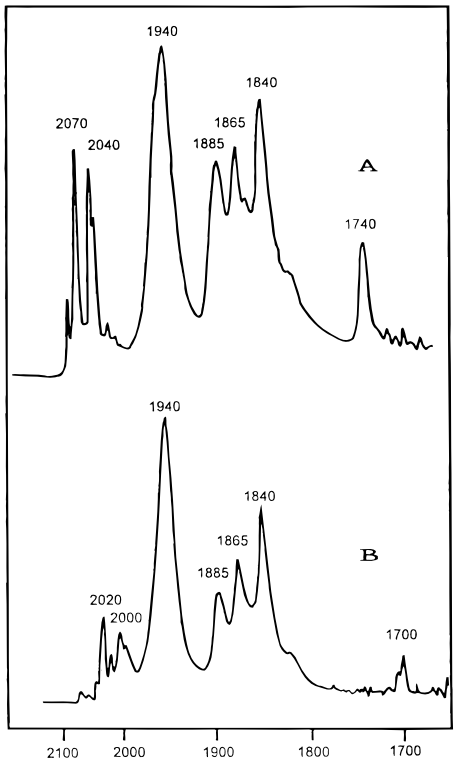

Figure 4. IR spectra (Nujol dispersion) of **IX** obtained by carbonylation of **I** or **II** with a blanket of CO (trace A) and of ^{13}CO (trace B). For experimental conditions, see the text.

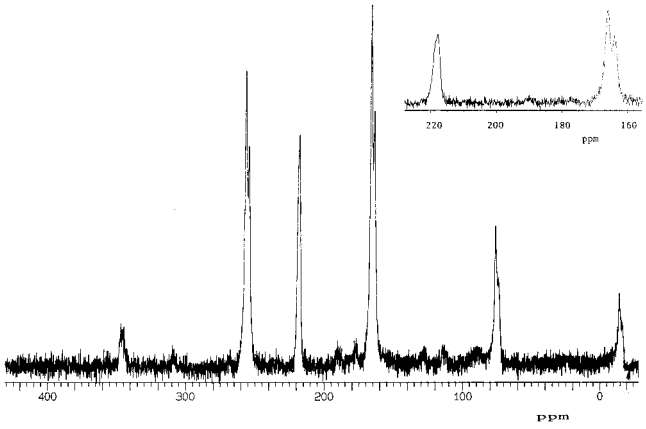

Figure 5. ^{13}C CPMAS NMR spectrum of species obtained by reacting complex **II** with ^{13}C-enriched CO. The inset shows the region of δ 230−160 ppm. For the experimental details, see Experimental Section.

added CO and that no exchange with those belonging to $Cr(CO)_3$ takes place. The presence of both terminal and bridged carbonyls bonded to iridium was confirmed by ^{13}C solid-state NMR measurements.

The high-resolution $\{^1H\}^{13}C$ solid-state spectrum of the product obtained using ^{13}CO as reagent is reported in Figure 5, and the inset shows the presence of three resonances at 217.9, 166.3, and 164.0 ppm in the relative ratio of 2:3:1, respectively. The low-field resonance falls in the typical range of bridging carbonyls bonded to iridium atoms whereas the two high-field resonances can readily be assigned to terminal carbonyls. Further support to this assignment arises from the spinning side-band analysis[13] that allows one to obtain the principal components for each resonance and then to evaluate their chemical shift anisotropy (csa)

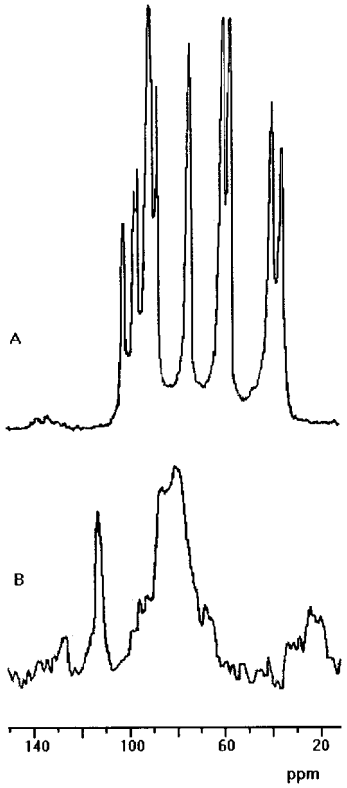

Figure 6. ^{13}C CPMAS NMR spectrum of complex **I** (trace A) and of product of its reaction with natural-abundance [^{13}C]CO (trace B). For the experimental details, see Experimental Section.

value. The computed values ($\Delta\sigma$ = 132 ppm for the signal at δ = 217.9 ppm and $\Delta\sigma$ = 365 ppm for the two peaks at δ 166.3 and δ = 164.0 ppm) are in the usual range found for csa of bridging and terminal carbonyls, respectively.[14]

In order to assess the hapticity mode of the indenyl group we performed a ^{13}C CPMAS spectrum of **IX** obtained by using natural-abundance [^{13}C]CO to avoid the intense spinning side-band manifold of the carbonyls (Figure 6, trace B), and we compared it with the ^{13}C solid-state spectrum of complex **I** (Figure 6, trace A). The reagent **I** shows 10 peaks at 99.3 (1 C), 93.7 (1 C), 92.6 (1 C), 85.4 (3 C's), 80.6 (1 C), 70.4 (2 C's), 56.0 (2 C's), 53.9 (2 C's), 37.1 (2 C's), and 30.7 (2 C's) ppm, respectively. Bearing in mind that inequivalences in the solid state can arise from the crystal packing, we assign on the basis of the solution spectrum (see Experimental Section) the four higher field resonances to the COD ligand and, among the other signals, the two peaks at 99.3 and 70.4 ppm to the C_2 and $C_{1,3}$ of the indenyl group. In the ^{13}C solid-state spectrum of the product obtained by reacting **I** with CO (lower trace), we observed the disappearence of the higher field resonances of the COD ligand, the formation of a broad hump centered at 80.2 ppm, and the presence of a sharper peak at 112.5 ppm. We tentatively assign this low-field peak to the C_2 atom of the indenyl group whereas the broad envelope of resonances centered at 80.2 ppm corresponds to a dispersion of the chemical

(13) Hawkes, G. E.; Sales, K. D.; Aime, S.; Gobetto, R.; Lian, L. Y. *Inorg. Chem.* **1991**, *30*, 1489. Hawkes, G. E.; Sales, K. D.; Gobetto, R.; Lian, L. Y. *Proc. R. Soc. London*, A **1989**, *424*, 93.
(14) Herzfeld, J.; Berger, A. E. *J. Chem. Phys.* **1980**, *73*, 6021.

shifts of the other aromatic carbons (On the basis of the available data we cannot exclude that the broadening feature has some contribution from slow motion of the ligand around its equilibrium position.).

On the basis of the IR and ^{13}C solid-state NMR data, we suggest the *syn* dimeric structure **IX** for this

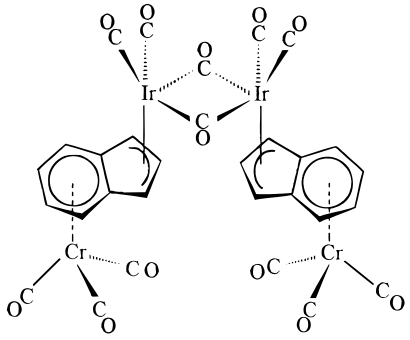

IX

precipitate, where the two indenyl moieties are located on the same side of the plane defined by the iridium atoms and the bridged carbonyls.

The η^3 hapticity mode of the iridium atoms to the indenyl ligand is justified on the basis of electron counting. The large downfield shift of the C_2 resonance ($\Delta\delta = 13.2$ ppm) found by comparing the NMR data for **IX** and **I** is in agreement with a change of the iridium hapticity from η^5 to η^3. [8b]

Iridium complexes where the metal is η^3-bonded to the cyclopentadienyl ring are not frequent; the only η^3-indenyl-IrL_3 species isolated and structurally characterized is that reported by Merola et al.,[10a] in which L = $PPhMe_2$, i.e., a strong σ-donor phosphine. Dimer **IX** is likely formed by rapid dimerization of the monomer intermediate **X**, an η^3 species likely very labile because

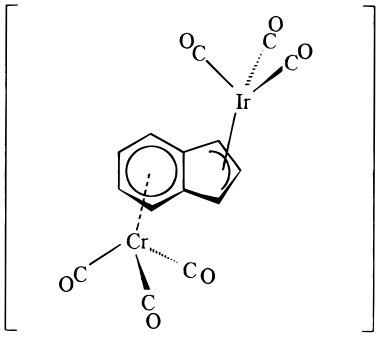

X

of the presence of strong π-acceptor ligands, viz., the CO's.

We believe that, under a blanket of CO, the reagent **I** is first quickly converted into the η^1-indenyl species **VI**; in the successive slow step, failing CO, the unstable **X** is formed, which quickly dimerizes to the scarcely soluble **IX**. Conversely, in presence of a large excess of CO the η^1-$Ir(CO)_4$ species, **VII** is formed.

The dimer **IX**, however, is stable only in the solid state. In fact, when it is dissolved in CH_2Cl_2 at 213 K, the initially observed IR spectrum (see Figure 2d) is very similar to that recorded in Nujol (Figure 4a); however, within a few minutes a new IR spectrum (Figure 2e) is

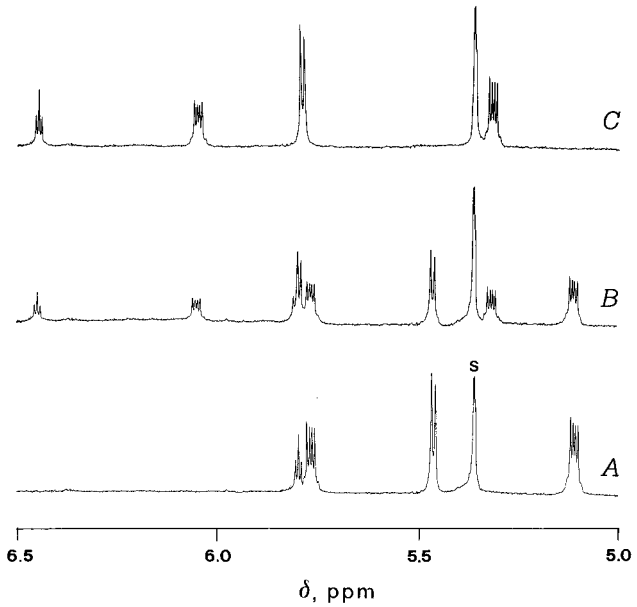

Figure 7. ^1H NMR spectra (solvent, CD_2Cl_2; T 283 K) of the process **XI** (trace A) → **III** (trace C): (A) $t = 0$; (B) t ~20 min; (C) $t = \infty$.

recorded. It exhibits two bands (2063 and 2030 cm^{-1}) due to Ir-bonded terminal carbonyls, two strong bands for the $Cr(CO)_3$ tripods at 1954 and 1881 cm^{-1}, and a weaker band at 1762 cm^{-1} due to bridging carbonyls, showing that a new complex, **XI**, is formed. This spectrum differs markedly from that of **III** (see Figure

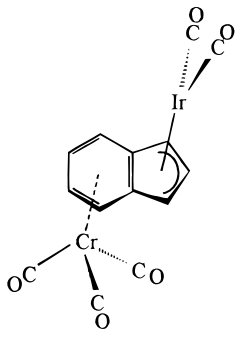

III

2f). In particular, the difference between the frequencies of the two stretching bands attributed to the terminal CO's is 33 cm^{-1} for **XI** and 66 cm^{-1} for **III**. The ^1H NMR spectrum of **XI** (Figure 7, trace A) is characteristic of an indenyl frame consisting of an AA′BB′ pattern at $\delta = 5.77$ and 5.11 ppm ($H_{4,7}$ and $H_{5,6}$, respectively) and a doublet at $\delta = 5.46$ ppm and a triplet at δ 5.86 ppm ($H_{1,3}$ and H_2, respectively) and is different from that of **III** (Figure 7, trace C). However, on raising the temperature to 273 K, both the IR and ^1H NMR spectra indicate that **XI** changes into **III**.

The changes of the ^1H NMR spectra due to the **XI** → **III** process are shown in Figure 7 for 283 K. The chemical shift values indicate that the indenyl protons of **XI** resonate at higher field with respect to the protons of complex **III**, the most significant upfield shift being shown by H_2. Therefore, the value of the parameter $\Delta\delta = \delta(H_{1,3}) - \delta(H_2)$, which was previously taken as a measure of the distortion from an η^5 hapticity toward

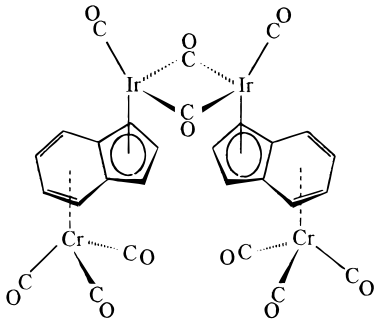

XI

η^3, [8b] decreases from 0.68 ppm for **III** to 0.40 ppm for **XI**, indicating a less distorted η^5 coordination in **XI** than in **III**. Thus, the IR and NMR data agree with the persistence of a dimeric structure in **XI** where the restoration of the η^5 hapticity is due to loss of two terminal CO's.

Intramolecular Rearrangements of VII. The ^{1}H NMR spectrum of η^1-[η^6-Cr(CO)$_3$-indenyl]-Ir(CO)$_4$ (**VII**) in methylene chloride solution manifests a marked temperature dependence (see Figure 8) suggesting the occurrence of intramolecular rearrangement processes. Stepwise increase in temperature from 233 to 273 K shows complete collapse of resonances relative to H_1 and H_3 along with change of the shape of the H_2 signal from a doublet of doublets to a triplet. This spectral behavior as well as the changes shown by the signals of the benzene ring protons can be explained by the occurrence of a [1,3]-shift of the Ir(CO)$_4$ group (a similar process involving the [Ir(CO)$_2$(COD)] group was shown for the analogous monometallic intermediate):[3]

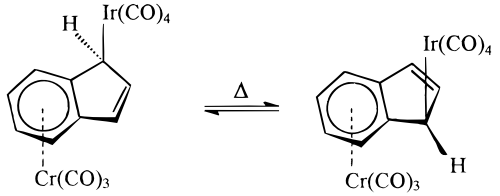

In addition, raising the temperature above 273 K induces further line broadening and, at 283 K, the complete collapse of all the resonances of the spectrum. At 293 K two broad signals at about δ 6.0 and 5.3 appear which at higher temperature change into a well-resolved AA′BB′ system due to $H_{4,7}$ and $H_{5,6}$ (at δ 5.98 and 5.25, respectively) corresponding to **III**. Also the resonances corresponding to H_2 and $H_{1,3}$, at δ 6.43 and 5.75, respectively, appear above 283 K, and the whole spectrum is identical to that recorded for complex **III**.

Additional information on intramolecular geometric changes of **VII** was obtained from the analysis of the IR spectra of the same solution recorded in the same temperature range. By raising the temperature above 203 K, the intensity of the bands corresponding to the iridium carbonyls of **VII** gradually decreases until complete disappearance at 298 K when they are replaced by four new bands at 2112, 2078, 2049, and 2034 cm^{-1} (see Figure 2c). In the same temperature range, no significant changes in the Cr(CO)$_3$ absorptions are observed. This behavior suggests the existence, above 273 K, of a dynamic process which changes the local

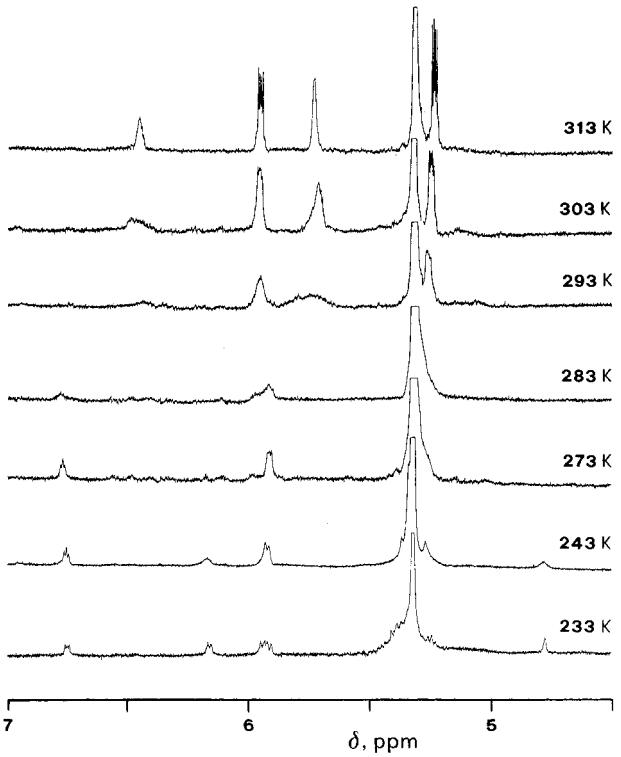

Figure 8. Temperature dependence of the ^{1}H NMR spectrum of **VII** in CD_2Cl_2. The signal at δ 5.32 is due to the undeuterated part of the solvent.

symmetry of the Ir(CO)$_4$ fragment, i.e., the interconversion of two stereoisomers, both having a bipyramidal trigonal structure, where the indene residue occupies either an axial or an equatorial coordinative position (Berry pseudorotation mechanism):

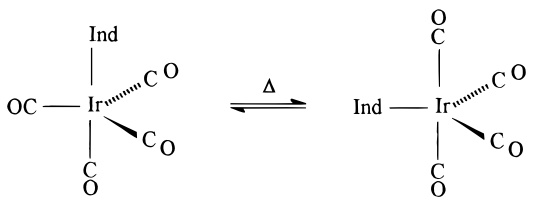

VII - ax **VII - eq**

In fact, the isomer stable at low temperature (**VII**-ax) exhibits three stretching bands relative to the carbonyls coordinated to iridium as required by the local symmetry C_{3v} of the Ir(CO)$_4$ group. Conversely, the four bands present in the spectrum of the isomer stable at higher temperature are consistent with the C_{2v} local symmetry of the Ir(CO)$_4$ group of the isomer **VII**-eq. In the spectrum recorded at room temperature (see Figure 2c), the additional strong single band observed at 2068 cm^{-1} is still unassigned.

Scheme 1 depicts the formation and the behavior of the species involved in the carbonylation reaction of the bimetallic complexes **I** and **II**. All the reported species except **X** have been spectroscopically detected and identified.

Conclusions

The carbonylation reaction of two heterobimetallic *anti*-[Cr(CO)$_3$-μ,η:η-indenyl-IrL$_2$] complexes (L$_2$ = COD;

Scheme 1. Proposed Mechanism for the Reaction of *anti*-[Cr(CO)$_3$-μ,η:η-indenyl-Ir(COD)] (I) and *anti*-[Cr(CO)$_3$-μ,η:η-indenyl-Ir(COE)$_2$] (II) with CO

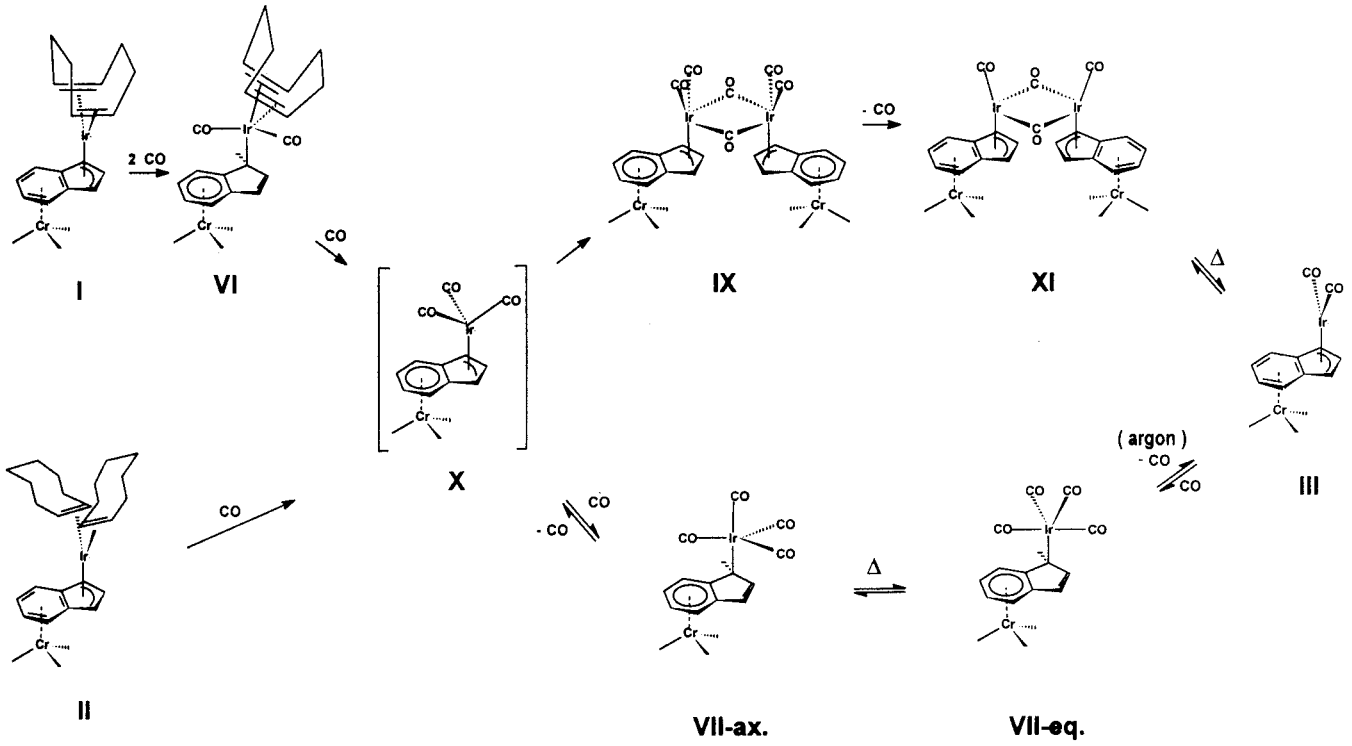

L = COE) has been studied under different experimental conditions. In the presence of a large excess of CO, the stepwise formation of stable η^1-[η^6-Cr(CO)$_3$-indenyl]-Ir(COD)(CO)$_2$ and η^1-[η^6-Cr(CO)$_3$-indenyl]-Ir(CO)$_4$ intermediates has been observed by NMR and IR spectroscopy. The rearomatization of the cyclopentadienyl ring is made difficult by the presence of the Cr(CO)$_3$ moiety and occurs only under forced conditions giving rise to the scarcely stable *anti*-[Cr(CO)$_3$-μ,η:η-indenyl-Ir(CO)$_2$] species. This behavior differs from that of the corresponding rhodium complexes, for which low-hapticity intermediates have been never detected, and where the carbonylation ends up with the formation of the stable "normal" substitution product, *anti*-[Cr(CO)$_3$-μ,η:η-indenyl-Rh(CO)$_2$].

On the other hand, at low CO concentrations, a poorly soluble iridium dimer, stable in the solid state, is obtained probably through the intermediacy of an unstable *anti*-[η^6-Cr(CO)$_3$-indenyl-η^3-Ir(CO)$_3$] species.

Experimental Section

Solution NMR spectra were measured on a Bruker AM400 spectrometer operating in the FT mode at 400.133 and 100.614 MHz for ^{1}H and ^{13}C, respectively. Chemical shifts are given in ppm from Me$_4$Si as internal standard. The ^3J(H,H) coupling constants, obtained from a first-order analysis, are given in hertz. The ^{13}C NMR peak assignment was based on selective proton decoupling experiments and partially relaxed spectra. The proton assignments were accomplished by ^{1}H−{^{1}H} NOE measurements: the usual procedure for gated experiments was modified,[15] and the selected multiplet was saturated by a 10-s cyclic perturbation of all lines with a 42-dB attenuation of a nominal 0.2-W decoupling power.

Solid-state ^{13}C NMR. High-resolution ^{13}C CPMAS NMR spectra were measured with Jeol GSE-270 and Bruker MSL-200 spectrometers operating at 67.8 and 50.5 MHz, respectively. In a typical experiment the CP contact time was 5 ms, the recycle time was 20 s, and the spinning speed was in the range from 3.5 to 6.0 kHz. For all samples, the magic angle was carefully adjusted from the ^{79}Br MAS spectrum of KBR by minimizing the line width of the spinning side-band satellite transitions.

IR spectra were run as CH$_2$Cl$_2$ solutions (optical length 0.2 mm, CaF$_2$ windows) on a Perkin Elmer 580B spectrophotometer equipped with a Perkin Elmer 3600 data acquisition system. The 70-eV EI mass spectra were recorded on a VG MicroMass-16 spectrometer.

All reactions were carried out in oxygen-free solution. Solvents were purified according to standard procedures,[16] distilled, and purged with argon before use. Commercial-grade COD and COE were twice distilled and deoxygenated before use.

η^5-Indenyl-Ir(COD) (V) and η^5-indenyl-Ir(CO)$_2$ were prepared as described in ref 6, and their IR and NMR data (in CD$_2$Cl$_2$ at 298 K) have been reported in ref 3.

***anti*-[Cr(CO)$_3$-μ,η:η-indenyl-Ir(COD)] (I).** Indene-Cr(CO)$_3$ (1.39×10^{-3} mol) in 15 mL of THF was metalated by treatment with an excess of KH at −40 °C under argon atmosphere.[7] The anion solution was added at −40 °C to an equivalent amount of [Ir(μ-Cl)(COD)]$_2$ in 25 mL of THF. After stirring for 1 h, the solvent was pumped off and the residue was extracted with diethyl ether and crystallized from diethyl ether−hexane to give deep red crystals. Yield, 60%. Mp, 155−160 °C dec. Anal. Calcd for C$_{20}$H$_{19}$CrIrO$_3$: C, 43.59; H, 3.52. Found: C, 43.55; H, 3.47. *m*/*z* 552 (M$^+$, based on ^{193}Ir). Spectroscopic data: IR ν_{max} (CH$_2$Cl$_2$): 1955 vs and 1872 vs cm^{-1} (C≡O). ^{1}H NMR (CD$_2$Cl$_2$): δ 6.17 (t, ^3J(H$_1$,H$_2$) = ^3J(H$_2$,H$_3$) = ∼2.8 Hz, 1H, H$_2$), 5.24 (d, 2H, ^3J(H$_1$,H$_2$) = ^3J(H$_2$,H$_3$) = ∼2.8 Hz, H$_{1,3}$), 6.08 and 5.23 (two multiplets, 2H each, AA′BB′ spin system, H$_{4,7}$ and H$_{5,6}$), 4.25 (m, 4H, =CH COD protons), and 1.78 (m, 8H, CH$_2$ COD protons). ^{13}C NMR (CD$_2$Cl$_2$) δ = 233.19 (C≡O), 94.72 (C$_2$), 69.713 (C$_{1,3}$), 84.91

(15) Kinns, M.; Sanders, J. K. M. *J. Magn. Reson.* **1984**, *56*, 518.

(16) Perrin, D. D.; Armageo, W. L. F. *Purification of Laboratory Chemicals*, 3rd ed.; Pergamon Press: Oxford, England, 1988.

Table 2. Summary of the Crystal Data and Intensity Collection for Indenyl-Ir(COD) (V), *anti*-[Cr(CO)$_3$-indenyl-Ir(COD)] (I), and *syn*-[Cr(CO)$_3$-indenyl-Ir(CO)$_2$] (IV)

	V	I	IV
formula	$C_{17}H_{19}Ir$	$C_{20}H_{19}CrIrO_3$	$C_{14}H_7CrIrO_5$
M	415.54	551.55	499.42
space group	C2/c	$P2_1/c$	$P2_12_12_1$
a/Å	15.704(2)	8.401(2)	12.388(2)
b/Å	6.421(2)	14.180(2)	16.535(2)
c/Å	26.754(3)	16.327(2)	6.612(1)
α/deg	90	90	90
β/deg	100.6(2)	95.9(2)	90
γ/deg	90	90	90
V/Å^3	2561.7(9)	1934.7(9)	1354(7)
Z	8	4	4
cryst dimens/mm	0.20 × 0.40 × 0.40	0.30 × 0.30 × 0.60	0.10 × 0.16 × 0.50
D_c, g cm^{-3}	2.08	2.02	2.45
μ/cm^{-1}	96.7	74.8	105.0
T, K	297	298	298
radiation (*λ*/Å)	graphite-monochromated Mo-Kα (*λ* = 0.7107)		
take-off angle/deg	3	3	3
scan speed/deg min^{-1}		2.0 in the 2*θ* mode	
2*θ* range/deg		3.0 ≤ 2q ≤ 45	
no. of unique reflctns [$F_o^2 = 2\sigma(F_o^2)$]	2888	3323	1749
R (on F_o)	0.058	0.061	0.063
F(000)	1583.6	1123.8	827.8
GOF	0.940	0.930	0.830

($C_{3a,7a}$), 84.43 ($C_{4,7}$), 90.20 ($C_{5,6}$), 54.12 (=CH COD carbon atoms), 33.00 (CH_2 COD carbon atoms).

***anti*-[Cr(CO)$_3$-*μ*,*η*:*η*-indenyl-Ir(COE)$_2$] (II)**. A solution of indene-Cr(CO)$_3$ (1.19 × 10^{-3} mol in 12 mL of THF) was converted into the corresponding anion by treatment with an excess of KH at −40 °C under argon atmosphere.[7] The anion solution was added at −40 °C to an equivalent amount of [Ir(*μ*-Cl)(COE)$_2$]$_2$ dimer in 22 mL of THF. After stirring for 1 h, the solvent was pumped off and the residue was extracted with diethyl ether and crystallized from diethyl ether−hexane to give a deep red powder. Yield, 42%. Mp, 110−115 °C dec. Anal. Calcd for $C_{28}H_{35}CrIrO_3$: C, 50.60; H, 5.31. Found: C, 50.64; H, 5.20. *m*/*z* 664 (M$^+$, based on ^{193}Ir). IR ν_{max} (CH_2Cl_2): 1954 vs and 1880 vs cm^{-1} (C≡O). ^{1}H NMR (CD_2Cl_2): *δ* 6.26 (t, 1H, $^3J(H_1,H_2) = {}^3J(H_2,H_3) = \sim$2.5 Hz, H_2), 5.02 (d, 2H, $^3J(H_1,H_2) = {}^3J(H_2,H_3) = \sim$2.5 Hz, $H_{1,3}$), 6.03 and 5.28 (two multiplets, 2H each, AA′BB′ spin system, $H_{4,7}$ and $H_{5,6}$), 2.09 (m, 4H, =CH COD protons), and 1.2−1.8 (m, 24H, $(CH_2)_6$ COD protons). ^{13}C NMR (CD_2Cl_2): *δ* 234.19 (C≡O), 97.66 (C_2), 76.59 ($C_{1,3}$), 86.85 ($C_{3a,7a}$), 85.532 ($C_{4,7}$), 90.83 ($C_{5,6}$), 56.97 (=CH COD carbon atoms), 26.7, 32.8, 33.5 (CH_2 COD carbon atoms).

***syn*-[Cr(CO)$_3$-*μ*,*η*:*η*-indenyl-Ir(CO)$_2$] (IV).** A suspension of freshly sublimated 3.5 × 10^{-3} mol of Cr(CO)$_6$ in 25 mL of CH_3CN was refluxed for 22 h under argon. After cooling to room temperature, the solvent was pumped off and the yellow Cr(CO)$_3$(CH_3CN)$_3$ obtained as a powder was dissolved at 25 °C in 8 mL of a THF solution of indenyl-Ir(CO)$_2$ (2.75 × 10^{-4} mol). After 5 h stirring, the precipitate formed was filtered, washed with THF, and then extracted with diethyl ether. After filtration on a silica column, the solvent was evaporated and the product obtained as a yellow powder. Yellow crystals were obtained by recrystallization from diethyl ether−hexane solution. Yield, 57%. Mp, 220−225 °C dec. Anal. Calcd for $C_{14}H_7CrIrO_5$: C, 33.61; H, 1.41. Found: C, 33.67; H, 1.41. *m*/*z* 499 (M$^+$, based on ^{193}Ir). IR ν_{max} (CH_2Cl_2): 2046 s and 1984 s cm^{-1} (Ir−C≡O), 1944 vs and 1895 vs cm^{-1} (Cr−C≡O). ^{1}H NMR (CD_2Cl_2): *δ* 6.48 (t, 1H, $^3J(H_1,H_2) = {}^3J(H_2,H_3) = \sim$2.8 Hz, H_2), 4.25 (d, 2H, $^3J(H_1,H_2) = {}^3J(H_2,H_3) = \sim$2.8 Hz, $H_{1,3}$), 4.35 and 5.42 (two multiplets, 2H each, AA′BB′ spin system, $H_{4,7}$ and $H_{5,6}$). ^{13}C NMR (CD_2Cl_2): *δ* 235.45 (Cr−C≡O), 171.92 (Ir−C≡O), 80.47 (C_2), 52.67 ($C_{1,3}$), 110.23 ($C_{3a,7a}$), 73.70 ($C_{4,7}$), 90.21 ($C_{5,6}$).

***η*^{1}-[*η*^{6}-Cr(CO)$_3$-indenyl]-Ir(CO)$_2$(COD) (VI)**. On bubbling precooled CO into a 10^{-2} M solution of **I** in CH_2Cl_2 cooled to 203 K, the color of the solution changes from orange to dark yellow in a few minutes. More concentrated solutions deposit an unstable yellow powder. IR ν_{max} (CH_2Cl_2): 2036.2 s and 1989.8 s cm^{-1} (Ir−C≡O), 1950.5 vs and 1870.1 vs cm^{-1} (Cr−C≡O). ^{1}H NMR (CD_2Cl_2, T 203 K): *δ* 6.80 (d, 1H, $^3J(H_1,H_2) = \sim$3.2 Hz, H_2), 6.10 (d, 1H, $^3J(H_1,H_2) = \sim$3.2 Hz, H_3), 6.09 (d, 1H, $^3J(H_6,H_7) = \sim$7 Hz, H_7), 5.95 (d, 1H, $^3J(H_4,H_5) = \sim$7 Hz, H_4), 5.38 (t, 1H, $^3J(H_4,H_5) = {}^3J(H_5,H_6) = \sim$7 Hz, H_5), 5.27 (t, 1H, $^3J(H_5,H_6) = {}^3J(H_6,H_7) = \sim$7 Hz, H_6), 4.11 and 3.99 (two multiplets, 2H each, olefinic COD signals), 3.30 (s, 1H, H1), 2.65 and 2.35 (two m, 8H overall, methylene COD protons). No ^{13}C spectra were obtained because of the low solubility of this species.

***η*^{1}-[*η*^{6}-Cr(CO)$_3$-indenyl]-Ir(CO)$_4$ (VII)**. The above mentioned solution of **VI** was warmed to 273 K. IR ν_{max} (CH_2Cl_2): 2118.3 s, 2051.4 s, and 1976.4 s cm^{-1} (Ir−C≡O), 1955.4 vs and 1876.4 vs cm^{-1} (Cr−C≡O). ^{1}H NMR (in CD_2Cl_2, recorded at 203 K to avoid the intramolecular dynamic processes described in the text): *δ* 6.75 (d, 1H, $^3J(H_1,H_2) = \sim$3 Hz, H_2), 6.15 (d, 1H, $^3J(H_1,H_2) = \sim$3 Hz, H_3), 5.98 (d, 1H, $^3J(H_6,H_7) = \sim$7 Hz, H_7), 5.90 (d, 1H, $^3J(H_4,H_5) = \sim$7 Hz, H_4), 5.40 (t, 1H, $^3J(H_4,H_5) = {}^3J(H_5,H_6) = \sim$7 Hz, H_5), 5.25 (t, 1H, $^3J(H_5,H_6) = {}^3J(H_6,H_7) = \sim$7 Hz, H_6), and 4.78 (br s, 1H, H_1). The spectrum also shows the signals of the uncoordinated COD at *δ* 5.57 (br s, 4H, olefinic protons) and *δ* 2.23 (s, 8H, methylene protons). No ^{13}C spectra were obtained because of the low solubility of this species.

***anti*-[Cr(CO)$_3$-*μ*,*η*:*η*-indenyl-Ir(CO)$_2$] (III).** This species was obtained (*i*) by bubbling argon for few minutes at room temperature through the above mentioned methylene chloride solution of **VII** or (*ii*) by warming the same solution at 313 K (some decomposition occurred in the last case). IR ν_{max} (CH_2Cl_2): 2051 s and 1987 s cm^{-1} (Ir−C≡O), 1962 vs and 1882 vs cm^{-1} (Cr−C≡O). ^{1}H NMR (CD_2Cl_2): *δ* 6.43 (t, 1H, $^3J(H_1,H_2) = \sim$2.6 Hz, H_2), 5.75 (d, 2H, $^3J(H_1,H_2) = {}^3J(H_2,H_3) =$ 2.6 Hz, $H_{1,3}$), 5.98 and 5.25 (two multiplets, 2H each, AA′BB′ spin system, $H_{4,7}$ and $H_{5,6}$). ^{13}C NMR (CD_2Cl_2): *δ* 232.55 (Cr−C≡O), 169.00 (Ir−CO), 106.80 (C_2), 69.71 ($C_{1,3}$), 90.65 ($C_{3a,7a}$), 84.03 ($C_{4,7}$), 91.29 ($C_{5,6}$).

[*η*^{6}-Cr(CO)$_3$-indenyl-*η*^{3}-Ir(CO)$_3$]$_2$ (IX). I (or **II**) (4.35 × 10^{-4} mol) dissolved in 8 mL of CH_2Cl_2 was stirred at room temperature under a blanket of CO. After a few minutes, the solution turned from orange to dark red and a yellow precipitate appeared. The reaction mixture was cooled to −20 °C; the solid product was recovered by filtration, washed with cold CH_2Cl_2, and dried under a stream of argon. Yield, 50%. Mp, 120−125 °C dec. Anal. Calcd for $C_{30}H_{14}Cr_2Ir_2O_{12}$: C, 34.16; H, 1.34. Found: C, 31.50; H, 1.55. IR ν_{max} (Nujol): 2090 w,

2070 vs, 2040 vs, 1746 sh, and 1740 s cm^{-1} (Ir−C≡O), 1950 sh, 1940 vs, 1885 vs, 1865 vs, and 1840 vs cm^{-1} (Cr−C≡O).

Crystallography. Crystals suitable for diffractometric analysis were obtained by slow solvent evaporation from concentrated solutions of **V**, **I**, and **IV** in methylene chloride. Crystal data, intensity data collection, and processing details are presented in Table 2. The data were obtained with a Philips PW-100 four-circle automated diffractometer with a graphite monochromator. Standard centering and autoindexing procedures indicated a monoclinic lattice for **V** and **I** and an orthorhombic one for **IV**. The orientation matrix and accurate unit cell dimensions were determined from angular settings of 25 high-angle reflections. Intensity data were collected at 25 °C using the 2θ scan method. Two reference reflections, monitored periodically, showed no significant variation in intensity. Data were corrected for Lorentz and polarization effects, and an empirical absorption correction was applied to the intensities (Ψ scan). The positions of Cr and Ir atoms were determined from the three-dimensional Patterson function. All the remaining atoms, including hydrogens, were located from successive Fourier maps using SHELX-76.[17] The crystal structure of **I** contains 0.5 mol of solvent (CH_2Cl_2) per mole of the complex. Its two chlorine atoms are symmetrically located around inversion centers at $^1/_2,0,^1/_2$ determining a statistical disorder of methylene groups spread out on a circle centered at $^1/_2,0,^1/_2$ and normal to the chlorine−clorine axis. Anisotropic thermal parameters were used for all the non-hydrogen atoms. Blocked-cascade least-squares refinements converged to R 0.058, 0.061, and 0.063 for **V**, **I**, and **IV**, respectively.

(17) Sheldrick, G, M. *SHELX-76*, Program for Crystal Structure Determination, Cambridge University: Cambridge, England, 1976.

Acknowledgment. This work was supported in part by the CNR, Roma, through its "Centro di Studio sugli Stati Molecolari Radicalici ed Eccitati" and through its Progetto Strategico "Tecnologie Chimiche Innovative".

Supporting Information Available: Tables giving the positional parameters of the non-hydrogen atoms, the anisotropic thermal parameters of the non-hydrogen atoms, the positional parameters of the hydrogen atoms, and full lists of bond lengths and angles for **I**, **IV**, and **V**, ^{1}H NMR spectra of **III** and **IV**, and ORTEP views of **I** and **V** (17 pages). Ordering information is given on any current masthead page.

OM9706065